10-1997

Electrode Performance Test on Single Ceramic Fuel Cells Using as Electrolyte Sr- and Mg-Doped $LaGaO_3$

Kevin Huang
University of South Carolina - Columbia, huang46@cec.sc.edu

Man Feng

John B. Goodenough

Christopher Milliken

Publication Info

Published in *Journal of The Electrochemical Society*, Volume 144, Issue 10, 1997, pages 3620-3624.

Publisher's Version: http://dx.doi.org/10.1149/1.1838058
Huang, K., Feng, M., Goodenough, J. B., & Milliken, C. (1997). Electrode Performance Test on Single Ceramic Fuel Cells Using as Electrolyte Sr- and Mg-Doped $LaGaO_3$. Journal of The Electrochemical Society, 144 (10), 3620 - 3624. http://dx.doi.org/10.1149/1.1838058

transference numbers were very high (nearly equal to 1). Average thermal expansion coefficients were higher than that of YSZ, ranging from 11.3 to 12.1 $\times 10^{-6}$ °C^{-1}.

Acknowledgments

The Pacific Northwest Laboratory is operated for the U.S. Department of Energy by Battelle Memorial Institute under Contract De-AC06-76RLO 1830.

The authors thank Nat Saenz, Shelley Carlson, Jim Young, Steve Paulik, Kate von Reis, John Darab, and A. S. Rupaal (Western Washington Unviersity) for their assistance with this work.

Manuscript submitted Feb. 19, 1997; revised manuscript received July 22, 1997.

Pacific Northwest National Laboratory assisted in meeting the publication costs of this article.

REFERENCES

1. H. Matsuda, T. Ishihara, Y. Mizuhara, and Y. Takita, in *Solid Oxide Fuel Cells III*, S. C. Singhal and H. Iwahara, Editors, PV 93-4, p. 129, The Electrochemical Society Proceedings Series, Pennington, NJ (1993).
2. T. Ishihara, H. Matsuda, Y. Mizuhara, and Y. Takita, *Solid State Ionics*, **70/71**, 234 (1994).
3. T. Ishihara, H. Matsuda, and Y. Takita, *J. Am. Chem. Soc.*, **116**, 3801 (1994).
4. T. Ishihara, H. Matsuda, and Y. Takita, in *Ionic and Mixed Conducting Ceramics*, T. A. Ramanarayanan, W. L. Worrell, and H. L. Tuller, Editors, PV 94-12, p. 85, The Electrochemical Society Proceedings Series, Pennington, NJ (1994).
5. T. Ishihara, H. Matsuda, and Y. Takita, *Solid State Ionics*, **79**, 147 (1995).
6. M. Feng and J. B. Goodenough, *Eur. J. Solid State Inorg. Chem.*, **31**, 663 (1994).
7. K. Huang, M. Feng, and J. Goodenough, *J. Am. Ceram. Soc.*, **79**, 1100 (1996).
8. A. Petric, P. Huang, and A. Skowron, in *Proceedings of 2nd European SOFC Forum*, Vol. 2, B. Thorstensen, Editor, p. 751, European SOFC Forum, Switzerland (1996).
9. P. Huang and A. Petric, *This Journal*, **143**, 1644 (1996).
10. L. A. Chick, L. R. Pederson, G. D. Maupin, J. L. Bates, L. E. Thomas, and G. J. Exarhos, *Mater. Lett.*, **10**, 6 (1990).
11. L. A. Chick, G. D. Maupin, G. L. Graff, L. R. Pederson, D. E. McCready, and J. L. Bates, *Mater. Res. Soc. Symp. Proc.*, **249**, 159 (1992).
12. J. C. Russ, *Practical Stereology*, Plenum, New York (1986).
13. R. S. Shannon, *Acta Crystallogr.*, **A32**, 751 (1976).
14. S. Srilomsak, D. Schilling, and H. Anderson, in *Proceedings of 1st International Symposium on SOFC*, S. Singhal, Editor, PV 89-11, p. 129, The Electrochemical Society Proceedings Series, Pennington, NJ (1989).
15. P. Kofstad, *Nonstoichiometry, Diffusion, and Electrical Conductivity in Binary Metal Oxides*, Krieger, Malabar, FL (1983).
16. P. Shewmon, *Diffusion in Solids*, 2nd ed., The Minerals, Metals, and Materials Society, Warrendale, PA (1989).
17. M. J. Verkerk, B. J. Middelhuis, and A. J. Burggraaf, *Solid State Ionics*, **6**, 159 (1982).
18. F. K. Moghadam, T. Yamashita, and D. A. Stevenson, in *Science and Technology of Zirconia*, A. H. Heuer and L. W. Hobbs, Editors, Advances in Ceramics, **3**, p. 364, American Ceramic Society, OH (1981).
19. M. Kleitz, H. Bernard, E. Fernandez, and E. Schouler, in *ibid.*, p. 310.
20. S. P. S. Badwal and M. V. Swain, *J. Mater. Sci. Lett.*, **4**, 487 (1985).
21. W. D. Kingery, H. K. Bowen, D. R. Uhlmann, *Introduction to Ceramics*, 2nd ed., Wiley, New York (1976).

Electrode Performance Test on Single Ceramic Fuel Cells Using as Electrolyte Sr- and Mg-Doped $LaGaO_3$

Keqin Huang,* Man Feng,* and John B. Goodenough

Center for Materials Science and Engineering, University of Texas at Austin, Austin, Texas 78712-1063, USA

Christopher Milliken**

Ceramatec, Incorporated, Salt Lake City, Utah 84119, USA

ABSTRACT

The electrode performance of a single solid oxide fuel cell was evaluated using a 500 μm thick $La_{0.9}Sr_{0.1}Ga_{0.8}Mg_{0.2}O_{2.85}$ (LSGM) as the electrolyte membrane. Comparison of $La_{0.8}Sr_{0.4}CoO_{3-\delta}$ (LSCo) and $La_{0.9}Sr_{0.1}MnO_3$ (LSM) as cathodes showed LSCo gave an exchange current density two orders of magnitude higher than that of LSM. Comparison of CeO_2/Ni and LSGM/Ni as anodes showed a degradation of the latter with time, and studies of the anode-electrolyte interface and the reactivity of NiO and LSGM suggest better anode performances can be obtained with a buffer layer that prevents formation of $LaNiO_3$. The cell performance showed that, with a proper choice of electrode materials and LSGM as the electrolyte, a SOFC operating at temperatures 600°C < T_{op} < 800°C is a realistic goal.

Introduction

The solid oxide fuel cell (SOFC) promises a high conversion efficiency (40 to 60%) of chemical energy to electric power with negligible pollution and is attractive for use in the cogeneration of electric power. The prototype SOFCs now being marketed use yttria-stabilized zirconia (YSZ) as the oxide-ion electrolyte, which forces an operating temperature $T_{op} \approx 1000$°C if conventional thick-film ceramic membranes are used. The interconnector between individual cells must be stable in both the oxidizing atmosphere at the cathode and the reducing atmosphere at the anode; and at $T_{op} \approx 1000$°C, it is necessary to use a conducting ceramic. However, even the ceramic of choice,[1] Ca-doped $LaCrO_3$, loses oxygen from the side exposed to the anodic atmosphere and gains oxygen on the side exposed to the cathodic atmosphere, which causes the interconnector membranes to warp. An operating temperature in the range 600°C < T < 800°C could allow the use of an oxidation-resistant stainless steel or another alloy as the interconnector material; it would also reduce operating costs, increase durability, extend service life, and permit more frequent cycling.

Two approaches to a T_{op} < 800°C are under active consideration: (*i*) reduction of the thickness of the YSZ electrolyte membrane to $l \leq 10$ μm and (*ii*) use of another solid

* Electrochemical Society Student Member.
** Electrochemical Society Active Member.

electrolyte having an oxide-ion conductivity at or below 800°C that is comparable to that of YSZ at 1000°C. The most promising traditional material for the second approach is CeO_2 doped with an alkaline-earth oxide MO, but reduction of Ce^{4+} to Ce^{3+} in the anodic gas introduces into the electrolyte an unwanted polaronic conduction. However, $La_{0.9}Sr_{0.1}Ga_{0.8}Mg_{0.2}O_{2.85}$, hereinafter referred to as LSGM, has recently been identified as a superior oxide-ion electrolyte;[2-5] it has an oxide-ion conductivity $\sigma_o \geq 0.10$ S/cm at 800°C, good chemical stability, negligible electronic conduction over a broad range of oxygen partial pressures, and a stable oxide-ion conductivity over time at 600°C in preliminary aging tests. In this paper we give a preliminary report on the performance of a single cell constructed with the LSGM electrolyte and standard electrode materials. The behaviors of the individual electrodes and the electrolyte were monitored with cyclic voltammagram in a three-electrode configuration. The tests show excellent electrolyte performance, but also problems with the electrode-electrolyte interfaces that need to be addressed.

Experimental

Sample preparation.—LSGM samples were made by solid-state reaction as previously described.[3] The required amounts of La_2O_3 (99.97%), $SrCO_3$ (99.9%), Ga_2O_3 (99.99%), and MgO (99.99%) were mixed intimately with the aid of acetone for 1 h and fired overnight at 1250°C. After regrinding, the powder was milled with agate beads in a polyethylene jar to reduce the particle size to less than 1 μm. Disks 2 in. in diam were cold-pressed and sintered at 1550°C for 6 h. Thick membranes (~500 μm) were obtained by grinding down the sintered disks with a diamond wheel. It is recognized that 500 μm is too thick for practical applications, but this configuration allows evaluation of the electrodes and the electrolyte/electrode interfaces.

Powder x-ray diffraction on pulverized sintered powders was made with a Philips diffractometer and Cu K_α radiation. Well-polished LSGM samples were thermally etched and their microstructure examined with a scanning electron microscope (SEM, JEOL/JSM-35C). The thermal-expansion coefficient (TEC) of an LSGM disk was measured with a Perkin-Elmer TMA7 thermal analyzer from room temperature to 850°C; the pellet densities were determined with a pycnometer (Micrometrics Accupyc 1330). Two-probe ac impedance spectroscopy with Pt electrodes was used to determine the electrical conductivity (grain + grain boundary) of the LSGM samples; the dc conductivity was measured with a standard four-probe method.

Fuel-cell construction.—Two cathode materials were used for comparison: $La_{0.6}Sr_{0.4}CoO_{3-\delta}$ (LSCo), which has high electron and oxide-ion conductivities,[6,7] and $La_{0.9}Sr_{0.1}MnO_3$, which has a good electronic conductivity and little oxide-ion conductivity.

The anodes were formed by the reduction of LSGM/NiO or CeO_2/NiO composites to give porous LSGM or CeO_2 with metallic Ni particles on the walls of the porous channels.

The overpotentials at both the cathode and the anode were monitored with reference electrodes constructed from the same materials and in the same way as the working electrodes; the cell configuration is shown in Fig. 1. The electrodes were fabricated on the two sides of the 500 μm thick electrolyte membrane by screen printing a slurry of an intimate mixture of electrode powder and organic binder (from Heraeus). After baking at 1125°C for 2 h, Pt meshes with Pt leads were fixed, with excess electrode paste to achieve good contact, on top of each electrode to act as current collectors. The effective electrode area was 2.5 cm^2. The cells were finally glass sealed into ZrO_2 tubes at 1100°C for 30 min; ZrO_2 has a thermal expansion coefficient close to that of LSGM. The glass sealant used was developed by Ceramatec, Inc.

The test cells were placed in the hot zone of a vertical furnace. Air was supplied directly to the cathode surface; water-moistened (at ~30°C) hydrogen was fed to the anode

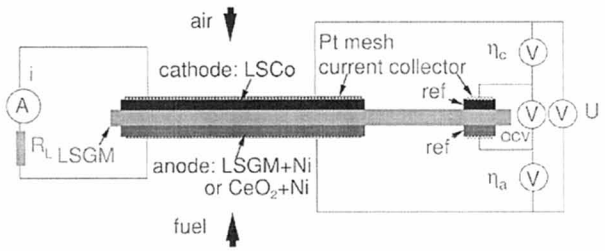

Fig. 1. Single fuel cell configuration.

surface at a rate of 100 ml/min. All the tests and the heating/cooling of the furnace were controlled by computer; the tests were carried out in the temperature range 600°C < T_{op} < 800°C. With a three-electrode configuration, cyclic voltammograms were taken at a fixed temperature from open-circuit voltage (OCV) to 0.4 V and back in steps of 20 mV and holding 10 s at each point.

Results and Discussion

The powder x-ray diffraction patterns of LSGM could be indexed into a primitive-cubic perovskite structure with a lattice parameter $a = 3.911$ Å; a small amount of $LaSrGaO_4$ was also detected as an impurity phase. The SEM observations revealed a preferential segregation of the granular-like second phase to the grain boundaries. (This observation shows that the LSGM electrolyte used did not have the optimal composition. We have found that removal of the second phase is possible and that its removal improves the electrolyte performance.) Table I lists the ac and dc conductivities of the LSGM samples, their measured density, and the thermal-expansion coefficient (TEC).

The fuel-cell configuration allowed separate measurements of the anode and cathode overpotentials, η_a and η_c, the *iR* voltage dropped across the electrolyte to obtain the area resistance *R* of the electrolyte, and the voltage drop ΔU between the reference and working electrodes from the cell terminal voltage *U*

$$U = U_{ocv} - \eta_a - \eta_c - iR - \Delta U \qquad [1]$$

where η_a, η_c, *iR*, and ΔU all increase with the cell current density *i*. The open-circuit voltage U_{ocv} at 800°C was typically 1.08 V, which is near the theoretical value and indicates negligible electronic conduction across the electrolyte.

Figure 2 shows the *i-V* and *i-P* curves obtained with an LSCo cathode and a CeO_2/Ni anode as measured in 50°C intervals from 600 to 800°C. The maximum power density of the cell is about 270 mW, which is 62% of the theoretical value 437 W/cm^2 (thickness: 500 μm, electrolyte conductivity 0.075 S/cm, OCV: 1.08 V). Even though about one-third of the power loss was spent on the electrodes, most of it on the anode (see discussion below), these results are still able to illustrate an excellent cell performance for a 500 μm thick LSGM membrane at a $T_{op} \geq 750$°C.

The voltage drop across the anode and cathode with respect to the corresponding reference electrodes gives η_a and η_c. LSCo has been identified as a promising cathode material despite its larger thermal expansion coefficient compared with that of LSGM. Figures 3 and 4 show, for a given temperature, an almost linear dependence on η_c and η_a on *i* for an LSCo/LSGM/CeO_2 + Ni test cell, which indi-

Table I. Some technical data for the LSGM samples measured in this study.

	AC conductivity (S/cm)			DC conductivity (S/cm)			Density (g/cm^3)	TEC (× 10^{-6} [K])
	600°C	700°C	800°C	600°C	700°C	800°C		20 ~ 850°C
LSGM	0.013	0.045	0.10	0.013	0.028	0.075	6.58	11.5

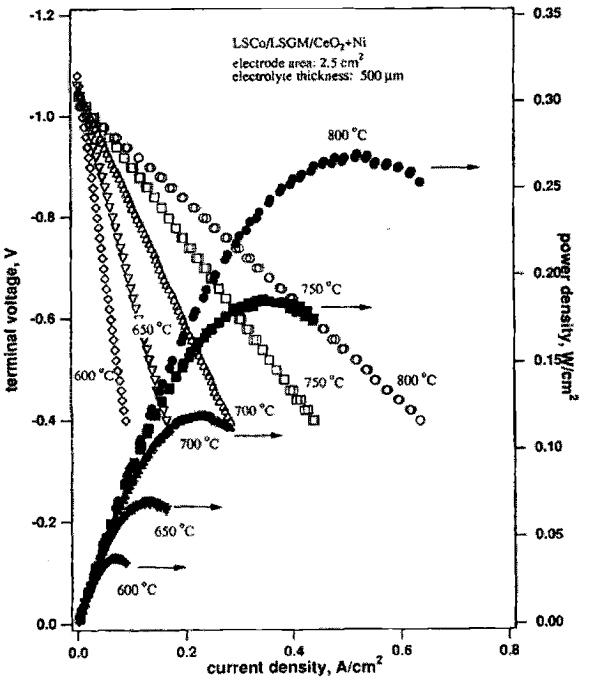

Fig. 2. Single fuel cell performance based on LSGM electrolyte with LSCo as cathode and CeO_2/Ni as anode at different temperatures.

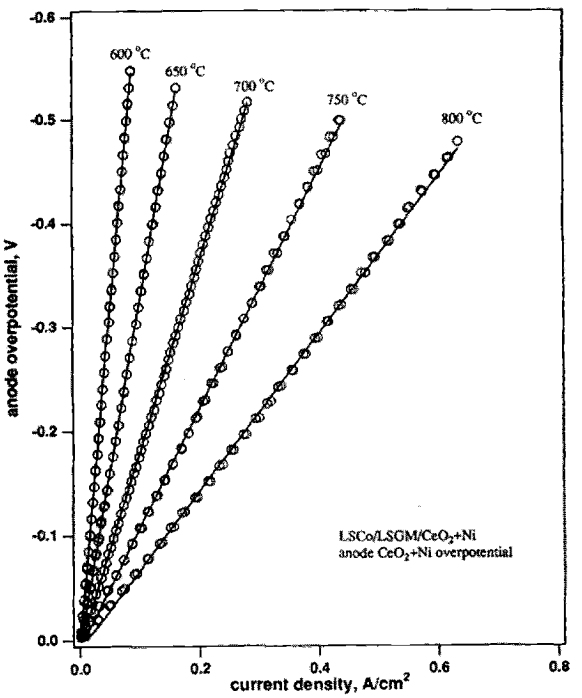

Fig. 4. Plot of anode CeO_2/Ni overpotential *vs.* current density.

cates a weak electrode polarization. The exchange current densities i° listed in Table II were obtained for each electrode from the slope of the equation

$$\eta = \frac{RT}{nFi^\circ} i \qquad [2]$$

where $n = 2$ is the number of charges transferred per oxide ion at the electrode/electrolyte interface. The high value of i°, *i.e.*, the low area electrode resistance, for the LSCo cathode is due to its good oxide-ion as well as electronic conduction, which allows utilization of the large surface area of the porous electrode for reduction of O_2 to 2 O^{2-}. As in the LSCo cathode, mixed electronic and oxide-ion conduction in the CeO_2-based anode increases the mass-transfer rate at the electrode surface and gives a low area electrode resistance below $i \leq 0.7$ A/cm^2. The higher anode overpotential observed suggests problems either with a structural mismatch at the interface or with a chemical interaction between LSGM and NiO (see discussion below).

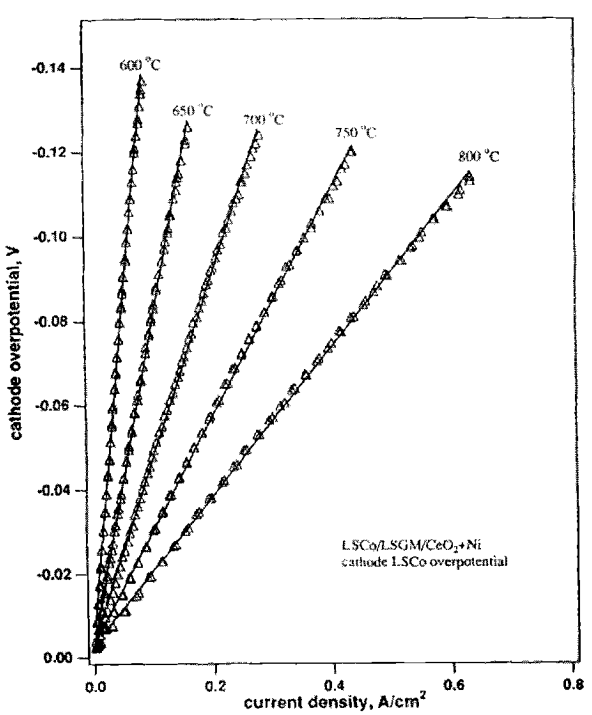

Fig. 3. Plot of cathode LSCo overpotential *vs.* current density.

$La_{1-x}Sr_xMnO_3$ (LSM) is at present the leading candidate material for the cathode of ZrO_2-based SOFCs operating at 1000°C. However, the oxide-ion conductivity of LSM is negligible under an oxidizing atmosphere, so a large three-phase (gas, electrode, electrolyte) boundary length is needed for charge and mass transfer to occur. Therefore, a porous, thick LSM coating was fabricated on the electrolyte membrane by screen printing. Figure 5 shows the performance of an LSM/LSGM/LSGM + Ni test cell; it is to be compared with that of an LSCo/LSGM/LSGM + Ni test cell shown in Fig. 6. A high η_c is found for the LSM cathode, and the shape of the η_c– i curve indicates that both oxygen diffusion and charge-transfer are limiting the performance of this cathode. The exchange-current density i° given in Table II was taken from the low-i portion of Fig. 5. The poor cell performance with LSM as cathode clearly indicates that LSM is an inappropriate cathode material for an LSGM fuel cell.

Table II. The exchange current density i° (A/cm^2) of the electrodes used in this study at different temperatures. The area electrode resistance (Ω cm^2) is shown in parenthesis.

T (°C)	LSCo	CeO_2/Ni	LSM
800	0.263 ± 0.001	0.061 ± 0.004	0.003 ± 0.001
	(0.175 ± 0.001)	(0.758 ± 0.049)	(15.4 ± 5.1)
750	0.164 ± 0.002	0.039 ± 0.004	—
	(0.269 ± 0.003)	(1.130 ± 0.115)	
700	0.097 ± 0.003	0.023 ± 0.005	—
	(0.432 ± 0.013)	(1.822 ± 0.396)	
650	0.052 ± 0.004	0.012 ± 0.008	—
	(0.764 ± 0.058)	(3.313 ± 2.208)	
600	0.024 ± 0.010	0.006 ± 0.015	—
	(1.567 ± 0.653)	(6.267 ± 5.667)	

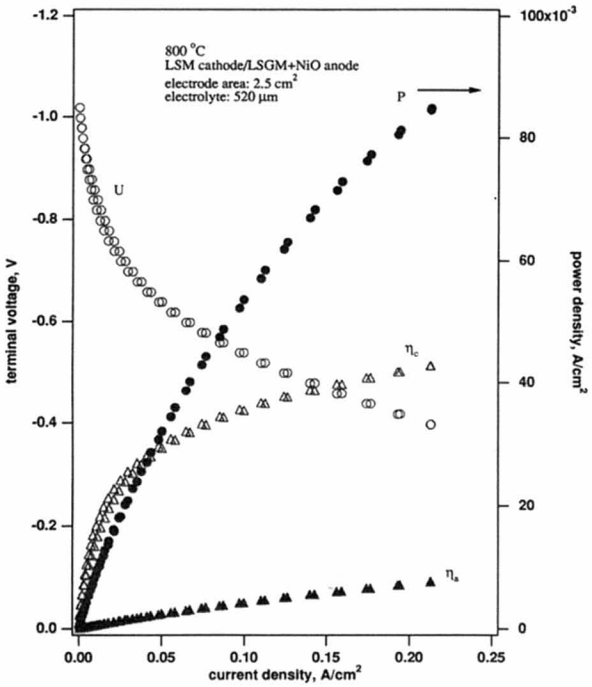

Fig. 5. Single fuel cell performance based on LSGM electrolyte with LSM as cathode and LSGM + Ni as anode at 800°C.

Table II shows that the exchange-current density i° at an LSCo cathode is nearly two orders of magnitude higher, the area electrode resistance correspondingly lower, than that at an LSM cathode. LSCo has not only a much higher oxide-ion conductivity than LSM, but also a high surface-oxygen exchange rate; and as noted by Steele,[10] the catalytic activity of a CeO_2/Ni anode is higher than that of a ZrO_2/Ni anode. On the other hand, comparison of Fig. 6 and Fig. 4 shows an initial η_a for an LSGM + Ni anode about half that for the CeO_2 + Ni anode of the cell. However, the performance of the LSGM + Ni anode degraded after cycling to a current density $i = 0.7$ A/m^2. A doubling of η_c at the LSCo cathode of the cell of Fig. 6 compared to that of Fig. 2 kept the maximum

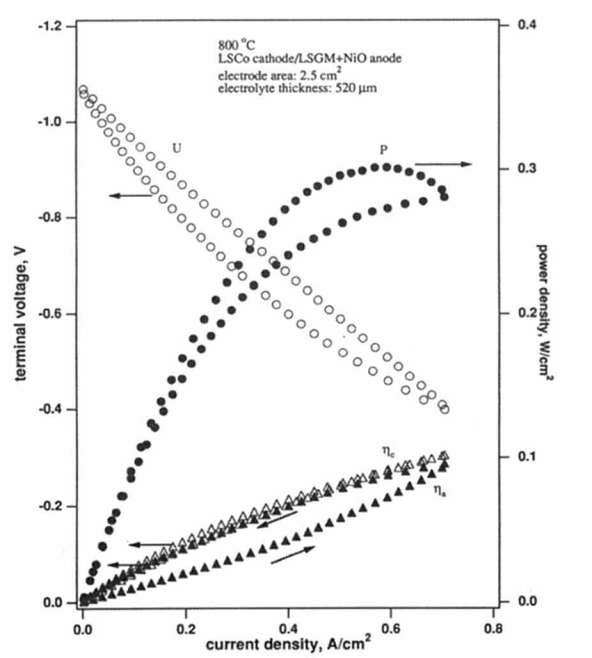

Fig. 6. Single fuel cell performance based on LSGM electrolyte with LSCo as cathode and LSGM + Ni as anode at 800°C.

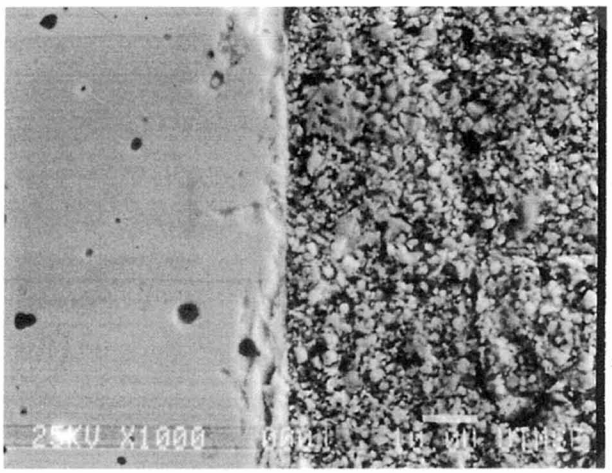

Fig. 7. Microstructure of LSGM/LSGM + Ni interface after testing.

power density at 800°C to 300 mW/cm^2, which is 70% of the theoretical value, compared to the 270 mW/cm^2 obtained with the cell of Fig. 2. The variation of η_c from cell to cell indicates that the process of cathode fabrication needs to be carefully controlled.

Figure 7 shows an SEM picture of the anode-electrolyte (LSGM + Ni anode) interface in cross section after testing. The anode remains well bonded, so the degradation in performance seems to imply either a coarsening of the Ni particles, which seems unlikely to be more rapid on LSGM than on CeO_2, or a reaction of the Ni with the LSGM to form $LaNiO_3$. We have found formation of $LaNiO_3$ at 1400°C. Although any $LaNiO_3$ present after firing a mixture of LSGM and NiO at 1125°C, the electrode preparation temperature, was not detectable by x-ray diffraction, nevertheless we have found that the introduction of a suitable interfacial layer prevents the increase of η_a with time and lowers the absolute value of η_a. The detailed results of this study will soon be published.

Conclusions

Single-cell SOFC tests with a 500 μm thick LSGM electrolyte show promising performance compared to a YSZ electrolyte at operating temperatures 600°C < T_{op} < 800°C. A steady and relatively high maximum power density was obtained with an LSCo cathode and a CeO_2 + Ni anode, but neither electrode can be considered optimal. The tests were able to demonstrate the superiority of a cathode that is a conductor of both oxide ions and electrons as compared to LSM, which is only an electronic conductor below 800°C. In the absence of a buffer layer, an anode containing Ni obtained by reduction of NiO reacts with an LSGM electrolyte to form $LaNiO_3$; this surface reaction degrades the catalytic conversion of 2 O^{2-} to O_2 followed by the reaction with hydrogen. These electrodes performance tests show that the realization of a SOFC operating in the range of 600°C < T_{op} < 800°C is a realistic goal with the LSGM electrolyte.

Acknowledgment

We thank Electric Power Research Institute (EPRI) for financial support with Contract 806028. Dr. Wate T. Bakker is the manager of this project.

Manuscript submitted March 3, 1997; revised manuscript received July 21, 1997.

The University of Texas at Austin assisted in meeting the publication costs of this article.

REFERENCES

1. I. Yasuda and T. Hikita, in *Proceedings of the 2nd International Symposium on Solid Oxide Fuel Cells*, F. Gross, P. Zegers, S. C. Singhal, and O. Yamamoto, Editors, pp. 645-652, Commission of the European Communities, Luxembourg (1991).

2. T. Ishihara, H. Matruda, and Y. Takita, *J. Am. Chem. Soc.*, **116**, 3801 (1994).
3. M. Feng and J. B. Goodenough, *Eur. J. Solid State Inorg. Chem.*, **31**, 663 (1994).
4. K. Q. Huang, M. Feng, and J. B. Goodenough, *J. Am. Ceram. Soc.*, **79**, 1100 (1996).
5. K. Q. Huang, M. Feng, J. B. Goodenough, and M. Schmerling, *This Journal*, **143**, 3630 (1996).
6. O. Yamamoto, Y. Takeda, R. Kanno, and M. Noda, *Solid State Ionics*, **22**, 241 (1987).
7. Y. Ohno, S. Nagata, and H. Sato, *ibid.*, **3/4**, 439 (1981).
8. J. H. Kuo, H. U. Anderson, and D. M. Sparlin, *J. Solid State Chem.*, **87**, 55 (1990).
9. M. J. L. Ostergärd and M. Mogensen, *Electrochim. Acta*, **38**, 2015 (1993).
10. B. C. H. Steel, *J. Power Sources*, **49**, 1 (1994).

Structure, Composition, and Morphology of Electrodeposited $Co_{0.9}Fe_{0.1}$(Cu) Alloys

E. M. Kakuno, N. Mattoso, W. H. Schreiner, and D. H. Mosca*

Departamento de Física, Universidade Federal do Paraná, Centro Politécnico, C. P. 19091, 81531-990 Curitiba, Paraná, Brazil

M. P. Cantão

Coordenadoria de P&D em Materiais, LAC-COPEL, C. P. 318, 80001-970 Curitiba, Paraná, Brazil

ABSTRACT

The successful use of the electrochemical process to produce compositional heterogeneous $Co_{0.9}Fe_{0.1}$(Cu) alloys is shown. Structure, composition, and morphology of the heterogeneous alloyed films, produced by the potentiostatic method, has been investigated by means of different techniques. Energy dispersive spectroscopy analyses reveal that the total amount of Co and Fe in the electrodeposits is strongly dependent on the Cu concentration in the plating solution at the potentiodynamic range investigated. The Co:Fe ratio does not change drastically due to Cu incorporation in the electrodeposits. It was also observed that by increasing the Cu content in the electrodeposits a granular morphology is obtained. Transmission electron microscopy was used to characterize the micromorphology and the heterogeneous composition of the alloys. The polycrystalline character of electrodeposits with a predominant face-centered cubic structure was characterized by using selected area electron diffraction and x-ray diffraction measurements.

Introduction

Heterogeneous or cluster-based alloys have recently prompted many investigations due to their interesting magnetic properties.[1-6] Among the many interesting properties of these materials is the so-called giant magnetoresistance phenomenon which promises practical application. Despite the extensive use of electrodeposited Co-Fe alloys to fabricate thin-film heads[7] and magnetic force microscope tips[8] due to their soft magnetic properties; only recently Chang and Romankiw[10] report on the successful electrodeposition of $Co_{0.9}Fe_{0.1}$/Cu multilayers with giant magnetoresistance.

Electrodeposition of heterogeneous alloys offers the great advantage of simplicity and cost. However, in order to optimize parameters, which control properties like giant magnetoresistance, a basic understanding of the physical properties of this system is essential.

In this work, we report on the preparation and characterization of thin films of heterogeneous Co-Fe alloys with different amounts of incorporated Cu. The influence of the incorporation of Cu on the morphology, composition, and structure of Co-Fe alloys was investigated in the range of relatively high cathodic overpotential and relatively high concentration. We have focused on the ranges mentioned above since they are currently used to produce magnetic nanostructures. The investigation of the electrodeposition of $Co_{1-x}Fe_x$ alloys is presented elsewhere.[10]

Experimental

All deposition experiments were performed with a stationary parallel plate electrode system consisting of a Pt disk counterelectrode, a saturated Ag/AgCl reference electrode, and a polished Cu disk as the working electrode. The Cu electrode consisting of disks with an area of 2.83 cm^2 was mechanically polished with 1 μm diamond paste, washed with distilled water, then chemically polished by successive rinses in 20% diluted H_2SO_4 and H_3PO_4, and then carefully washed in distilled water immediately before each experiment. An EG&G PAR potentiostat/galvanostat (Model 273A) was used to control the potential in the depositions through an analog-digital converter fast interface board (4 μs) installed in a personal computer. The plating solutions were prepared from reagent grade chemicals ($CoSO_4$, $FeSO_4(NH)_2SO_4$, and $CuSO_4$) immediately prior to each experiment by dissolving the requisite amount of the metal sulfates in distilled water. Plating solutions with total concentrations from 1 to 0.02 *M* were prepared maintaining a proportion 9:1 molar of metallic ions from Co sulfate and Fe ammoniac-sulfate, respectively. The potentiostatic electrodeposition of alloys was carried out at room temperature without presence of additives (the pH was not adjusted). Each deposition was performed during 90 s monitoring the current through the cell by an oscilloscope (Hewlett-Packard, TDS320).

All results shown and discussed in this work were obtained from the central area (area: 0.79 cm^2) of the Cu disks with an approximate thickness of 0.3 μm. The thickness uniformity of the electrodeposit was determined by using a stylus profiler being not inferior to 50%.

Cathodic potential was increased continuously from 0 up to −1.60 V (V *vs.* Ag/AgCl reference is used hereafter) with a scan rate of 20 mV/s and steps of 2 mV. Curves of cathodic current *vs.* potential were used to optimize the electrodeposition conditions. Deposits made at −1.2 V present a metallic aspect for low Cu partial concentrations in the plating solutions. Deposits made with high Cu partial concentration present an opaque surface by visual inspection.[10] All the samples were deposited at cathodic potential of −1.2 V with cathodic currents varying from 75 to 250 mA.

* Electrochemical Society Active Member.